Monitoring Recent Lake Variations Under Climate Change Around the Altai Mountains Using Multimission Satellite Data

Rong Luo, Qiangqiang Yuan, *Member, IEEE*, Linwei Yue, and Xiaogang Shi, *Member, IEEE*

***Abstract*—Estimating lake dynamics is vital for the accurate evaluation of climate change and water resources monitoring. However, it remains a challenge to estimate the lake mass budget due to extremely scarce *in situ* data, especially for alpine regions. In this article, multimission remote sensing observations were blended to examine recent lake variations and their responses to climate change around the Altai Mountains during 2001–2009 and 2010–1018. First, the multitemporal Landsat images were used to enable the detailed monitoring of the surface extent of 43 lakes (> 5 km^2) around the Altai Mountains from 2001 to 2018. The results presented that the total lake surface extent shrunk from 9835 km^2 in 2001 to a minimum of 9652 km^2 in 2009, while subsequently rose to 9714 km^2 in 2018. By combining the lake area with the water level derived from the ICESat and CryoSat-2 altimetry data, the water storage of seven lakes covering $\sim$84% of the overall lake area in the region was obtained. The total water storage was detected with a decrease of 4.86 ± 1.17 km^3 from 2003 to 2009 and a decrease of 3.65 ± 1.16 km^3 from 2010 to 2018, respectively. Although most of the glaciers in this region had a significant mass loss in the past decades, the factor analysis indicated that most of the lakes had maintained a steady or slightly changing tendency because the glacial melting water was counteracted by the negative impact of high evapotranspiration amount. For the lakes with a few glacier melting supplies, e.g., the Uvs lake and Hyargas lake, the significant water budget loss was caused by the increasing evapotranspiration, decreased precipitation, and developed animal husbandry, which mainly dominated the overall decreasing trend of lake water storage in the Altai Mountains.**

***Index Terms*—Climate change, multimission satellite data, lake dynamic, water storage.**

I. Introduction

THE Altai mountains are important water conservation areas, which are located in the north of the Xinjiang Uygur autonomous region and western Mongolia, and extend to northwestern Russia, spanning China, Mongolia, Russia, and Kazakhstan [1]. The Altai mountains contain a large number of glaciers covering an area of 1191 km^2 [2], [3] and an abundant source of lakes [4]. The lakes distributed around the Altai mountains are a keystone of the terrestrial surface freshwater resource and are sensitive to the global climate variation. Studies have shown that the rapid retreat of glaciers, changing precipitation patterns, and anthropogenic activities characterized by irrigation, the establishment of the artificial reservoir, and groundwater exploitation have made a great impact on lakes [5]. The glaciers in the Altai mountains have shown a rapid decaying tendency in the western region in the past decades [1], [4], [6], [7]. The total glacier meltwater from the entire Altai mountains was 401.1×10^8 m^3 from 1990 to 2011, which was four times as much as the average annual discharge of the Irtysh River Basin [4]. Such a large supply of meltwater is extremely important for the freshwater input in the entire Altai mountains, particularly for arid zones. However, the extent to which the glacial change has affected the lakes around the Altai mountains is unclear. The accurate estimation of the changing trends of lakes in reaction to climate change and human activities is of great significance for understanding the water circulating process and reasonable protection of water resources [8], [9]. Nevertheless, few studies have provided a comprehensive discussion about the lake dynamics in the Altai mountain region.

Satellite remote sensing provides a chance for refined monitoring and estimation of the dynamics of the alpine lakes, especially for the remote regions that are lack of *in situ* data. Optical remote sensing images, such as the Landsat TM/ETM+ [10], [11], Huanjing satellites [12], [13], and GF-1 [14], can capture changes over longer periods, which have made an important contribution in monitoring the dynamics of surface extent in some typical lakes. The satellite altimetry data have been used to retrieve the lake water level time series in numerous studies [15]–[20]. For example, Li *et al*. [18] used the ICESat altimetry data to extract the temporal and spatial characteristics of lake elevation changes in Central Asia from 2003 to 2009. Song *et al*. [20] constructed a long time series of water level changes in the Nam Co Lake, by combining ICESat with Cyrosat data. Zhang *et al*. [19] quantified the lake elevation of 74 lakes distributed across the Tibetan Plateau (TP) and their changes using the ICESat altimetry data. Besides, the gravity recovery and climate experiment (GRACE) data have been used to estimate the

Manuscript received July 7, 2020; revised October 8, 2020; accepted October 25, 2020. Date of publication November 4, 2020; date of current version January 6, 2021. This work was supported by the National Natural Science Foundation of China under Grant 41801263. *(Corresponding author: Linwei Yue.)*

Rong Luo is with the School of Geodesy and Geomatics, Wuhan University, Wuhan 430072, China (e-mail: luorong96@whu.edu.cn).

Qiangqiang Yuan is with the School of Geodesy and Geomatics, Wuhan University, Wuhan 430072, China, and also with the Collaborative Innovation Center of Geospatial Technology, Wuhan University, Wuhan 430072, China (e-mail: qqyuan@sgg.whu.edu.cn).

Linwei Yue is with the School of Geography and Information Engineering, China University of Geosciences, Wuhan 430074, China (e-mail: yuelw@cug.edu.cn).

Xiaogang Shi is with the School of Interdisciplinary Studies, University of Glasgow, DG1 4ZL Dumfries, Scotland (e-mail: john.shi@glasgow.ac.uk).

Digital Object Identifier 10.1109/JSTARS.2020.3035872

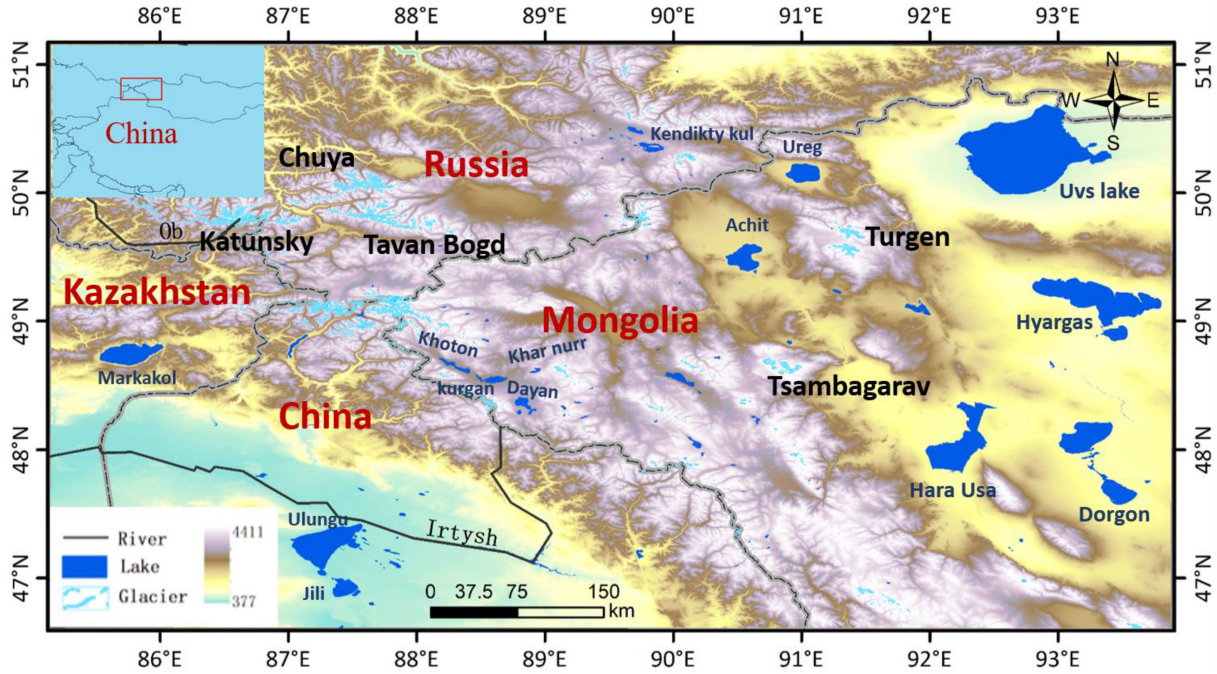

Fig. 1. Location and topography of the study region.

terrestrial water storage (TWS) anomaly in numerous regions across the globe [21]–[25]. However, a single data source cannot satisfy the demand for a comprehensive analysis of lake dynamics. Researchers have combined multisource remote sensing data, e.g., altimetry data, optical remote sensing images, and gravity data to monitor the lake changing mechanism [5], [26]–[28]. For example, Song *et al*. [29] obtained the elevation and surface extent of typical TP lakes using the data obtained from ICESat and Landsat series and verified TWS changes derived from GRACE. Moore and Williams [30] used the Envisat altimetry data, global land data assimilation system (GLDAS) hydrological model data, and GRACE gravity data to investigate the TWS anomaly in Africa from 2003 to 2011.

Our study aimed to investigate the dynamics of lakes around the Altai mountains from 2001 to 2018 and the driving forces of their changes by combining multimission remote sensing data. First, the interannual variations of the lake area and elevation around the Altai mountains were derived from optical satellite images and altimetry data. Then, the water storage variations of seven lakes were estimated based on the empirical equations between the water level and lake area. The GRACE product was used to validate the obtained water storage changes. Furthermore, the spatial and temporal trends of lakes were analyzed and the dominant factors were identified.

The rest of this article was organized as follows. Following the introduction, Section II described the study area and materials. Section III presented the data processing and analysis method. The results of lake surface extent, water level, and lake water storage changes for several lakes were presented in Section IV. Section V analyzed and discussed the effects of climatic factors, glacier melting, and human activities on lake change patterns. The conclusions were summarized in Section VI.

II. Study Area and Materials

A. Study Area

The study region, as shown in Fig. 1, rises from an altitude of 2000 m in northwest Altai to over 4500 m in the central region of the Altai mountains. Lakes are concentrated in the northern region of Xinjiang, the western plateau of Mongolia, and the eastern areas of Kazakhstan. Glaciers are distributed mainly in the Katunsky Mountain, Tavan Bogd Mountain, and Chuya Mountain [7]. The Altai mountains are an important climate boundary where climate modes vary between the southern and northern region, which is reflected in the different precipitation tendency in different regions [32]. The summer westerly circulation and winter Siberian High have an impact on climate change in the study area [33]. In summer, the westerly circulation brings the Atlantic water vapor and drives straight into the Altai mountains along the Erqisi valley and the Zaisan valley of Kazakhstan, which results in precipitation. The Altai mountains block the humid masses transported by the westerlies, which may result in a northwest to southeast precipitation gradient [34]. In winter, the high air pressure blocks the westerly winds because the study area is near to the center of the Siberian High, leading to an extremely cold and dry environment. This prevents the precipitation of the Mongolian western region in winter [35].

With the increase in land development and industrial water consumption in the upper reaches of the Ulungu river, it will lead to water shortage in the lower reaches and even the phenomenon of a flow interruption, bringing new impacts to the fragile ecological environment, so people made many projects to divert water from the Irtysh river [36]. In the western part of the Mongolian plateau, where mining and animal husbandry are booming, the population is increasingly dependent on lake supplies.

B. Materials

1) Optical Satellite Images: A total of 252 scenes of the Landsat TM/ETM+ images were used to extract the lake surface extent covering the study area from 2001 to 2018, which can be downloaded from the U.S. Geological Survey website[1]. All the images selected contain less than 10% of the cloud. Considering the influence of seasonal factors on the interannual variation of the lake area, the acquisition period of the image was limited from July to October of each year. Meanwhile, data gaps in the Landsat 7/ETM+ SLC-OFF images were filled based on the interpolation (triangulation) using a simple toolbox (Landsat Gapfill) on the ENVI software.

2) Satellite Altimetry Data: The altimetry data used to obtain the lake elevation variations were from ICESat's Level 2 global land-surface altimetry data product (GLA14) released by the National Snow and Ice Data Center from 2003 to 2009 and the CryoSat-2 Level 2 GDR data provided by the European Space Agency (ESA) from 2010 to 2018. ICESat observations have undergone a series of corrections, including the atmosphere and geodetic corrections. The narrow primary peak threshold retracker was applied to the CryoSat-2 data, which provided valid results for the inland water application [20].

3) Satellite Gravimetric Data: The gridded GRACE TWS anomaly products ($1° \times 1°$) are based on the RL05 spherical harmonics from the Jet Propulsion Laboratory, Centre for Space Research at the University of Texas at Austin, and the German Research Centre. GRACE's mission ended in October 2017 with a failure and GRACE Follow On was successfully launched in May 2018. Considering the gap between two missions, we only use GRACE data to validate the obtained water storage changes. The mean value of the three products was calculated to obtain the mean annual TWS change rate. The time series of the data for the three solution methods was collected from April 2002 to January 2017 with the data spanning a total of 159 months. For the data with voids, they were interpolated by averaging the values of two months before and after. The gravimetric data have undergone a series of correction [37]–[39], including the gravitational field changes, first-order coefficients, glacial isostatic adjustment, measurement and leakage errors, scale factor, the application of 300-km Gaussian filter smoothing radius, and replacement of C_{20} using satellite laser ranging observations. The GRACE data were used to validate the obtained water storage changes in this study.

4) Temperature and Precipitation Dataset: Temperature and precipitation are important indicators for understanding climate change. We used the University of Delaware (UDel) dataset provided by the NOAA/OAR/ESRL PSD, Boulder, CO, USA, to obtain temperature and precipitation changes in the study region. The UDel dataset is a monthly and globally gridded dataset ($0.5° \times 0.5°$) for air temperature and precipitation [61]. The dataset was obtained by interpolating the high-resolution station air temperature values and rain gage-measured precipitation values, respectively. The accuracy level of the dataset has been validated by several studies [54], [55] and widely applied to some hydrological research [58]–[60].

[1][Online]. Available: https://earthexplorer.usgs.gov/

5) Global Land-Surface Data Assimilation System Data: The GLDAS aims to combine satellite-based and ground-based observational data products using advanced land-surface modeling and data assimilation techniques to generate optimal land-surface conditions and flux fields [40]. The GLDAS provides global forcing data for four land-surface models: Noah, Mosaic, the variable infiltration capacity, and the community land model. The GLDAS dataset can provide hydrological variables with a high temporal and spatial resolution of 0.25°, and thus, they have been widely used in previous hydrological studies [41], [42]. In this article, the GLDAS potential evapotranspiration data from the Noah model were used to identify the relationship between the potential evapotranspiration (ET_P) and lake variation from 2001 to 2018 in the study region. This product has had good applicability for basin hydrology and energy studies [56], [57].

III. Methods

A. Estimating Lake Surface Extent

The method of extracting the lake area was derived from the normalized difference water index, which is based on the principle that the water body has a higher reflectance in the blue band and a low reflectance in the near-infrared band [43]. The thresholds were determined through trial and error and the initial extracted results were compared with google earth images using the visual interpretation. Some misclassified water bodies and the other small lakes were removed through manual editing based on the global lakes and wetlands database. Finally, the mapping results are visually examined and manually edited to ensure mapping accuracy.

To assess the uncertainty of extracting lake extents in this study, the Landsat image-delineated lake boundaries were compared with the extracted surface extent from the high-resolution images of google earth [44], and the results were presented in Appendix A. A total of 24 samples were randomly selected to illustrate the accuracy of lake mapping. The mapping accuracy was evaluated with the overall accuracy, the kappa coefficient, and the uncertainty. The uncertainty was calculated as the percentage of area difference. The comparison indicated that the uncertainty of Landsat image-delineated lake surface area was generally less than 2.5% for small lakes with the uncertainty of large lakes and medium lakes less than 0.8%.

B. Estimating Lake Water Level

ICESat altimetry data need to be converted from TOPEX reference ellipsoid to WGS84 reference ellipsoid to be consistent with the CryoSat-2 data before extracting it from the water mask [45]. Based on the extracted water surface extent from Landsat images, the data that completely fell into the extent of the lake was selected. As the data may be affected by clouds and terrain shadows, the obvious outliers were eliminated through visual interpretation first and the two-sigma criteria were used twice to discard the remaining gross errors. To reconstruct the water level variation for a longer period, the altimetry data derived from the ESA's CryoSat-2 Level 2 GDR altimetry products were also used to obtain the water level from 2010 to 2018. Reconstruction was implemented using the ESA basic radar altimetry toolbox [46].

The elevation data from October were used to be consistent with the water surface extent, as illustrated in Section III-A [18].

C. Estimating Lake Water Storage Variation

Several ways are generally used to estimate the lake water storage variation, such as using empirical equations based on the relationship between lake water level and the lake area [29] or estimating from the underwater topography [47]. In our study, we used the formula that combines the altimetry-derived water level and Landsat-interpreted surface extent to estimate the lake water storage change [48]

$$\Delta \boldsymbol{V} = \frac{\boldsymbol{1}}{\boldsymbol{3}} (\boldsymbol{H}_2 - \boldsymbol{H}_1) \times \left(\boldsymbol{A}_1 + \boldsymbol{A}_2 + \sqrt{\boldsymbol{A}_1 \times \boldsymbol{A}_2} \right) \quad (1)$$

where ΔV was the water volume change from the lake elevation H_1 and the area A_1 to the elevation H_2 and the area A_2. By combining the lake area with the water level derived from the ICESat and CryoSat-2 altimetry data, the total water volume variation from 2003 to 2009 and from 2010 to 2018 was obtained, respectively.

As for the accuracy level of the estimated lake water volume, according to the error propagation law, the uncertainty of the lake water volume change was calculated by (2). Meanwhile, the uncertainty of the lake area was 2.5% for the small lake and 0.8% for the large or medium lakes, while the standard deviation of the water level from ICESat and Cyrosat altimetry data was 20 cm

$$\sigma_{\Delta V_{\mathbf{Lake}}} = \sqrt{\begin{array}{l} \frac{\boldsymbol{1}}{\boldsymbol{9}} (\boldsymbol{A}_1 \boldsymbol{A}_2 + \boldsymbol{A}_1 + \boldsymbol{A}_2)^2 \left({\sigma_{\boldsymbol{H}_1}}^2 + {\sigma_{\boldsymbol{H}_2}}^2 \right) \\ + \frac{\boldsymbol{1}}{\boldsymbol{36}} (\boldsymbol{H}_2 - \boldsymbol{H}_1)^2 \left[\left(\frac{\boldsymbol{A}_2}{\boldsymbol{A}_1} + \boldsymbol{1} \right)^2 {\sigma_{\boldsymbol{S}_1}}^2 + \left(\sqrt{\frac{\boldsymbol{A}_1}{\boldsymbol{A}_2}} + \boldsymbol{1} \right)^2 {\sigma_{\boldsymbol{S}_2}}^2 \right] \end{array}}. \quad (2)$$

D. Mann–Kendall Trend Test

The Mann–Kendall test is a widely used nonparametric statistical test method [49] for analyzing the changing trends of lakes and climate factors. The advantage is that the selected sample does not need to comply with specific distribution and the test results are not affected easily by a few abnormal values. It is suitable for long-term-sequence trend mutation testing. Let x_1, …, x_n be the datapoint, for all $k, j \leq n$, and $k \neq j$, the test statistic S is calculated, and the formula is as follows:

$$\boldsymbol{S} = \sum_{\boldsymbol{k}=1}^{\boldsymbol{n}-1} \sum_{\boldsymbol{j}=\boldsymbol{k}+1}^{\boldsymbol{n}} Sgn\left(\boldsymbol{x_j} - \boldsymbol{x_k}\right) \quad (3)$$

and

$$Sgn\left(\boldsymbol{x_j} - \boldsymbol{x_k}\right) = \begin{bmatrix} +1 \left(\boldsymbol{x_j} - \boldsymbol{x_k}\right) > 0 \\ 0 \left(\boldsymbol{x_j} - \boldsymbol{x_k}\right) = 0 \\ -1 \left(\boldsymbol{x_j} - \boldsymbol{x_k}\right) < 0 \end{bmatrix} \quad (4)$$

where S is normally distributed and the mean value of which is zero; thus, the variance is given by

$$\mathbf{var}(\boldsymbol{s}) = \boldsymbol{n}(\boldsymbol{n}-\boldsymbol{1})(\boldsymbol{2n}+\boldsymbol{5})/\boldsymbol{18}. \quad (5)$$

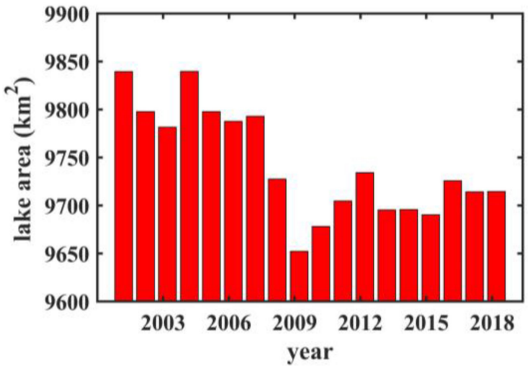

Fig. 2. Total lake area in the study area from 2001 to 2018.

When n is greater than 10, the standard normal distribution variable is calculated as follows:

$$\boldsymbol{Z} = \begin{bmatrix} \frac{\boldsymbol{S}-\boldsymbol{1}}{\sqrt{\mathbf{var}(\boldsymbol{S})}} \boldsymbol{S} > 0 \\ 0 \\ \frac{\boldsymbol{S}+\boldsymbol{1}}{\sqrt{\mathbf{var}(\boldsymbol{S})}} \boldsymbol{S} < 0 \end{bmatrix}. \quad (6)$$

In this work, the time series of the lake area and the climate data were used to analyze the corresponding significance level using this method. For statistic Z, if $|Z|$ is greater than 1.28, 1.96, and 2.31, a significant trend change exists in the series corresponding to a p-value of 0.1, 0.05, and 0.01, respectively.

IV. Results

A. Overview of Lake Area Change

A total of 43 lakes (>5 km^2) around the Altai mountains were investigated using the TM and ETM+ images from 2001 to 2018. Detailed information for the lake area was provided in Appendix B. Fig. 2 showed the total lake area variations obtained from the Landsat series between 2001 and 2018. The overall lake area in the study region shrunk from 9835 km^2 in 2001 to 9714 km^2 in 2018, while the nadir was 9652 km^2 in 2009 followed by a rebound since 2010. The results showed that more than half of the lakes maintained a steady and insignificant upward or downward trend with a changing rate (the regression coefficient between the year from 2001 to 2018 and the corresponding lake area) of less than 0.1 km^2/year (Fig. 3). The surface extent of 11 lakes showed a significant decreasing trend ($p < 0.05$). Conversely, six lakes' area in the northern region of the Xinjiang Uygur autonomous region experienced a significant expansion from 2001 to 2018.

To analyze the climate change effect on different-size lakes, the lakes were divided into small, medium, and large lakes. For that, we calculated the lake area change ratios from 2001 to 2018 to analyze the climate change effect on different-size lakes. The statistic from Fig. 4 revealed that the average area change ratios of two large lakes were 3.5%, while the average area change ratios of the medium and small lakes were 0.88% and 13.5%, respectively. The small lakes seemed to be more sensitive to the external change and showed the largest area change ratios.

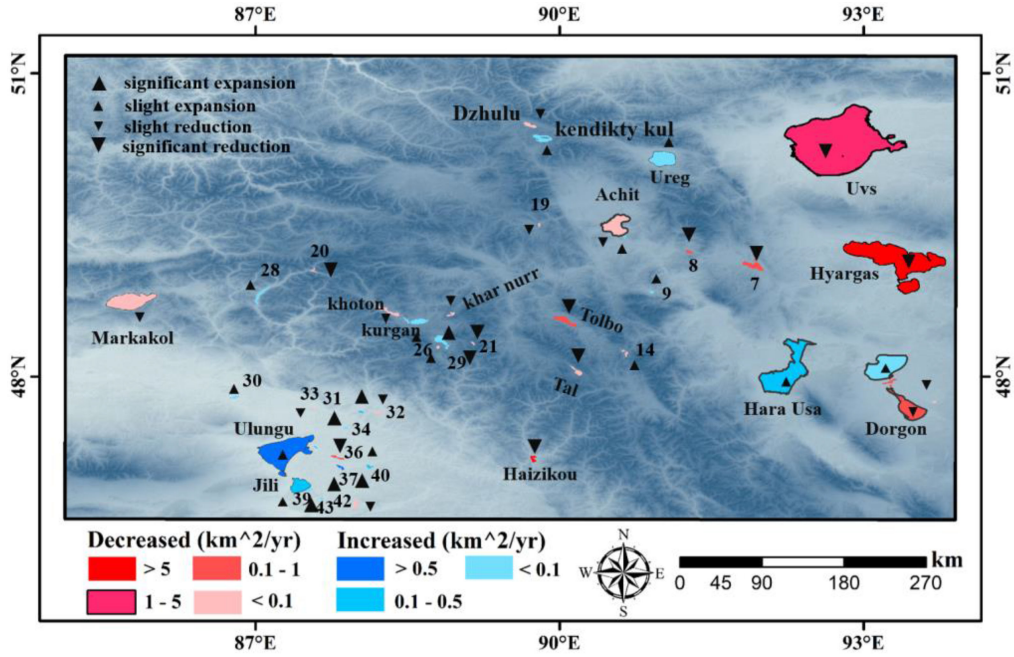

Fig. 3. Mean annual lake area change rate of 43 lakes during the period of 2001–2018.

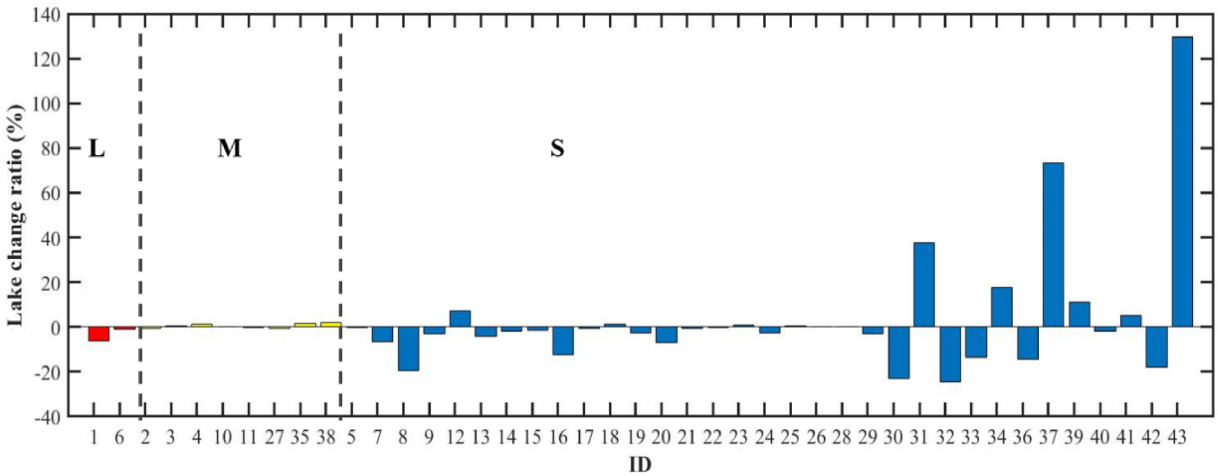

Fig. 4. Area change ratio for the small, medium, and large lake.

To better analyze the reasons for lake area variation, the lakes were further divided into the alpine closed lake, exorheic lake, reservoir, and plain terminal lake based on the geographical position, topography, and climate characteristics (see Fig. 5). Fig. 6 showed the lake area change rate of different types' lakes from 2001 to 2018. There were 18 alpine closed lakes distributed in the study area, the surface extent of which showed a decreasing trend on the whole. Exactly, among the alpine close lakes, 67% (12/18) of the lakes showed a decreasing trend and eight lakes had a significant shrinkage ($p < 0.05$), which were mainly distributed in the western arid region of the Mongolian plateau. The typical examples were the Uvs (ID: 1) and Hyargas lake (ID: 6), which were featured by a reduction of 34.05 km^2 and 95.61 km^2 during the analyzed period, respectively. The total decreasing trend of the lake area throughout the study region was attributed to the significant surface extent attenuation of the two lakes to a large extent. In Fig. 7, we gave the changing tendency of lake areas in this region excluding Uvs and Hyargas. When the two large lakes with continued shrinkage were not taken into account, the changing tendency of the whole lake area showed a similar trend, where the lowest lake area was obtained in 2009.

As shown in Fig. 6(b), there were ten exorheic lakes involved in area change monitoring, and most of them showed no significant upward or downward trend from 2001 to 2018. The Dorgan lake (ID: 4) suffered the largest area shrinkage rate (0.29 km^2/year) in all exoheric lakes. Nevertheless, its attenuation was not significant from 2001 to 2018 according to the M–K test. A similar tendency was observed in two exoheric lakes,

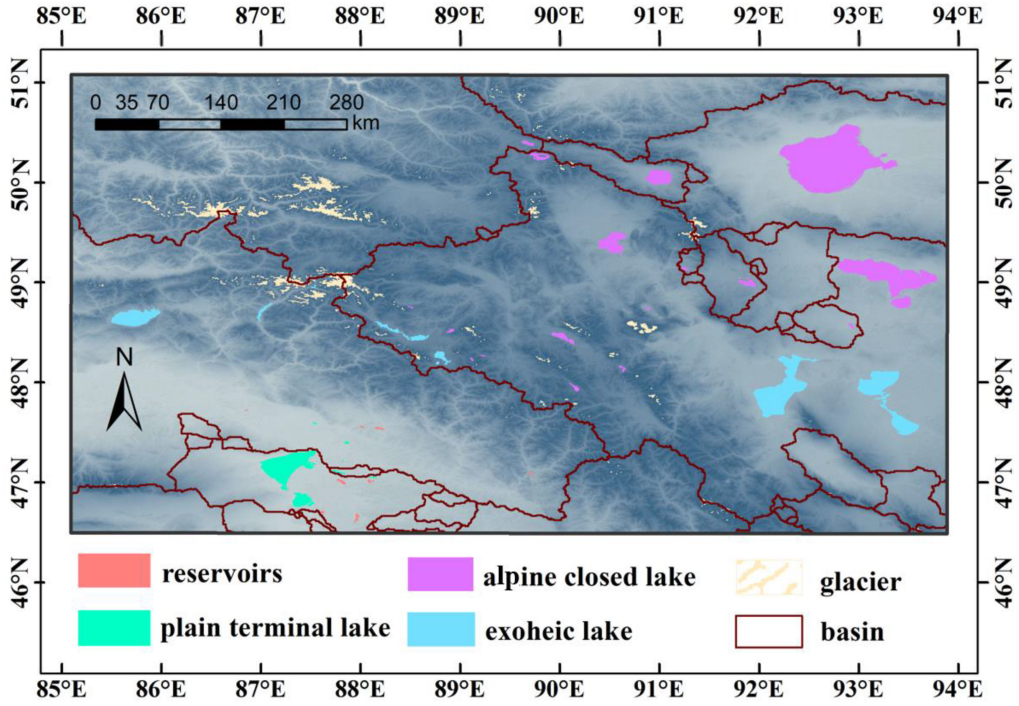

Fig. 5. Spatial distribution of four different types of lakes across the study region.

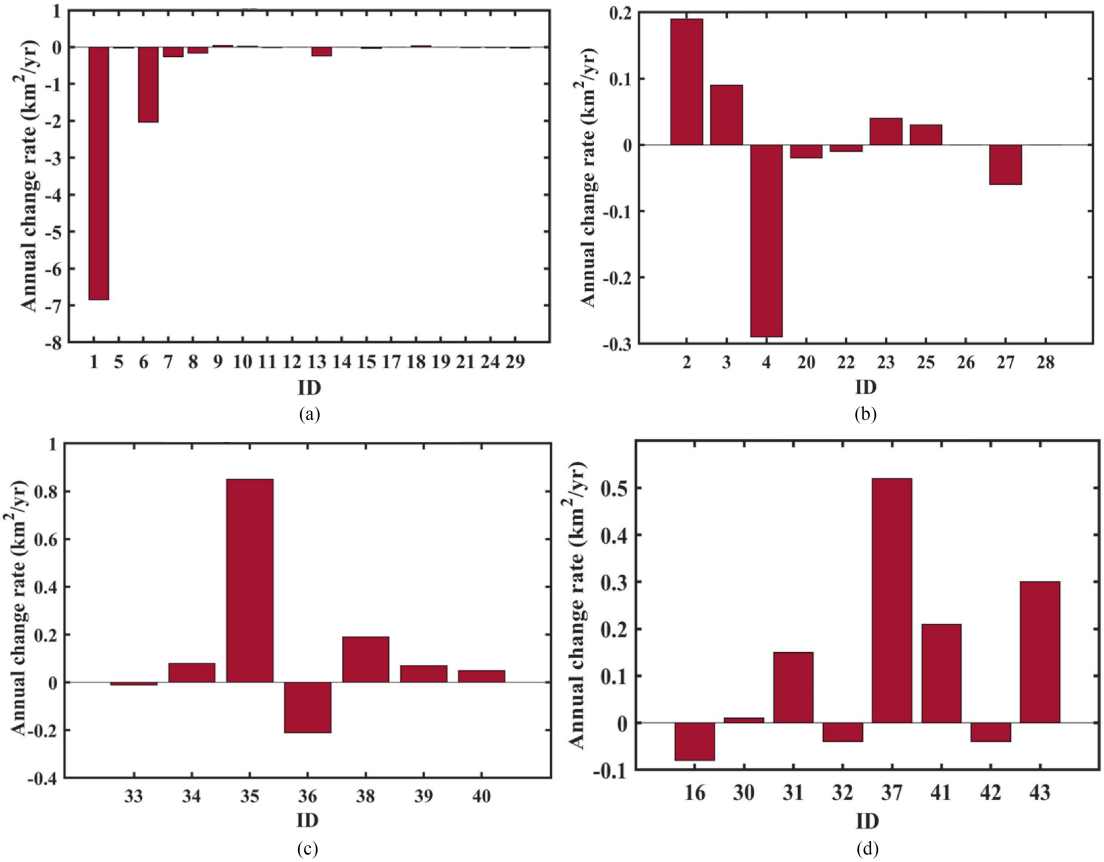

Fig. 6. Lake area change rate of different types from 2001 to 2018. They are 18 alpine closed lakes, 10 exorheic lakes, 7 plain terminal lakes, and 8 reservoirs. The ID number corresponding to the lakes can be referred to in Tables IV and V. (a) Alpine closed lake. (b) Exorheic lake. (c) Plain terminal lake. (d) Reservoir.

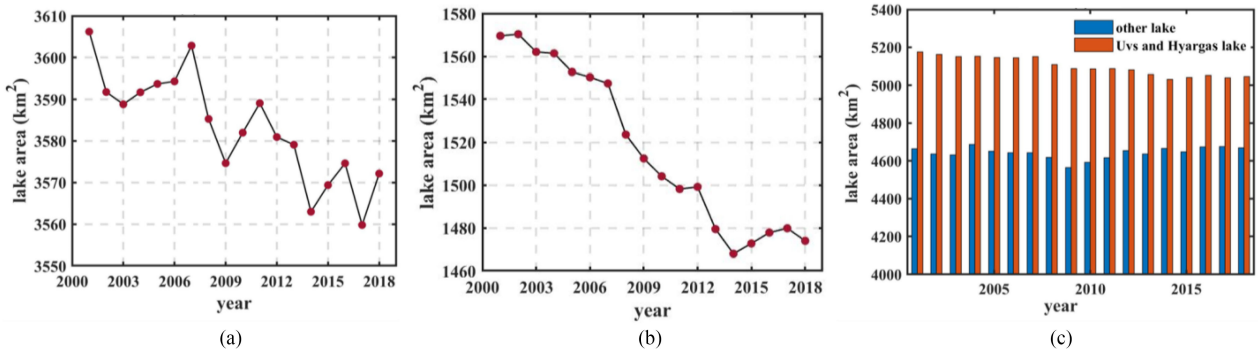

Fig. 7. Lake area of (a) Uvs lake, (b) Hyargas lake, (c) both Uvs and Hyargas lakes, and the other 41 lakes from 2001 to 2018.

Hara Nurr (ID: 3) and Hara Usa (ID: 2), which are connected to the Dorgan lake.

Besides, seven plain terminal lakes were mainly distributed in the southern part of the study region. Only two plain terminal lakes showed a slightly declining trend, while the other lakes suffered a slight expansion from 2001 to 2018. For instance, the two largest plain terminal lakes, Ulungu (ID: 35) and Jili (ID: 38), have shown a slightly increasing trend at the rate of 0.8 and 0.2 km^2/year, respectively.

Eight reservoirs were distributed in the southern part of the study region. More than half of these reservoirs showed an increasing trend. The surface extent of the reservoirs showed a large interannual amplitude during the analyzed period.

B. Annual Variations of Water Level and Water Storage

The annual water level and water storage variations of seven lakes with sufficient data points were obtained for the analysis. Fig. 8 presented the annual water level variation for the seven lakes measured by ICESat (2003–2009) and CryoSat-2 (2010–2018), respectively. Moreover, the water storage in the respective period was given in Table I. The lake extent of the seven lakes covered 84% of the overall lake area in the region. By combining the lake area with the water level derived from the ICESat and CryoSat-2 altimetry data, the total water storage was detected with a decrease of 4.86 ± 1.17 km^3 from 2003 to 2009 and a decrease of 3.65 ± 1.16 km^3 from 2010 to 2018, respectively. The water storage showed a negative balance during the studied period. Hyargas experienced the most significant shrinkage, the water level of which has decreased by 0.36 m/year with a water storage reduction of 3.36 ± 0.44 km^3 during 2003–2009 and 2.27 ±0.42 km^3 during 2010–2018. The plain terminal lake, Ulungu lake, in northern Xinjiang maintained a positive water storage budget. It suffered a slight shrinkage from 2003 to 2009 with the water level dropped by 0.3 m and then experienced a rising water level of 1.1 m from 2010 to 2018. The other exorheic lakes showed a slight water storage variation on the whole.

C. Link Between the Lake Water Storage Change and TWS Anomaly Derived From GRACE

The annual mean TWS anomaly from 2003 to 2016 was derived from the GRACE gravity data, as shown in Fig. 9. The GRACE data were mainly used to verify the obtained water volume changing trend. The GRACE TWS variation was consistent with the changing trend of lake water storage in some regions. For example, the reduced TWS estimated from GRACE was concentrated in the Mongolian plateau of the study region, where Hyargas and Uvs also suffered strong water storage shrinkage. In the northern part of Xinjiang, the lake water storage, such as in Ulungu and Jili, showed a significantly increasing trend, while the mass variation derived from GRACE also demonstrated an increased tendency.

V. Analysis and Discussion

A. Influence of Relative Climate Element and Human Activities on Lake Changes

The Altai mountains are located in an ecological transition region ranging from semidesert to humid landforms. The region is an important climate boundary where climate variation is different between the southern and northern Altai [32]. We analyzed the precipitation from 2001 to 2017 due to the lack of UDel precipitation data in 2018. The precipitation variation showed spatial heterogeneity, which decreased from southwest to northeast. Over 70% of the study region has experienced a slightly increasing trend of precipitation with a rate of 1.98 mm/year, which occurred in the western region of the study area from 2001 to 2017 (see Fig. 11). The precipitation for the rest of the study area (e.g., the western Mongolian plateau) displayed a decreasing trend with a declining rate of 1.35 mm/year from 2001 to 2017. We analyzed the correlation between the several significant changed lakes with the climate factors (i.e., precipitation, temperature, and potential evapotranspiration) (see Table II). Although the precipitation and lake area showed the same spatial variation trend, there was no significant correlation between the lake area and precipitation (except Hulagash). It indicated that the precipitation was not the reason for the most significant changed lake during the analyzed period.

Besides, lake evapotranspiration is the main discharge for most of the lakes, especially for the alpine closed lake and plain terminal lake. Table II also illustrated that several large alpine closed and plain terminal lakes had a significant negative correlation with the potential evapotranspiration. For example, the correlation coefficient between the Uvs lake and potential evapotranspiration was -0.52. A significant negative correlation

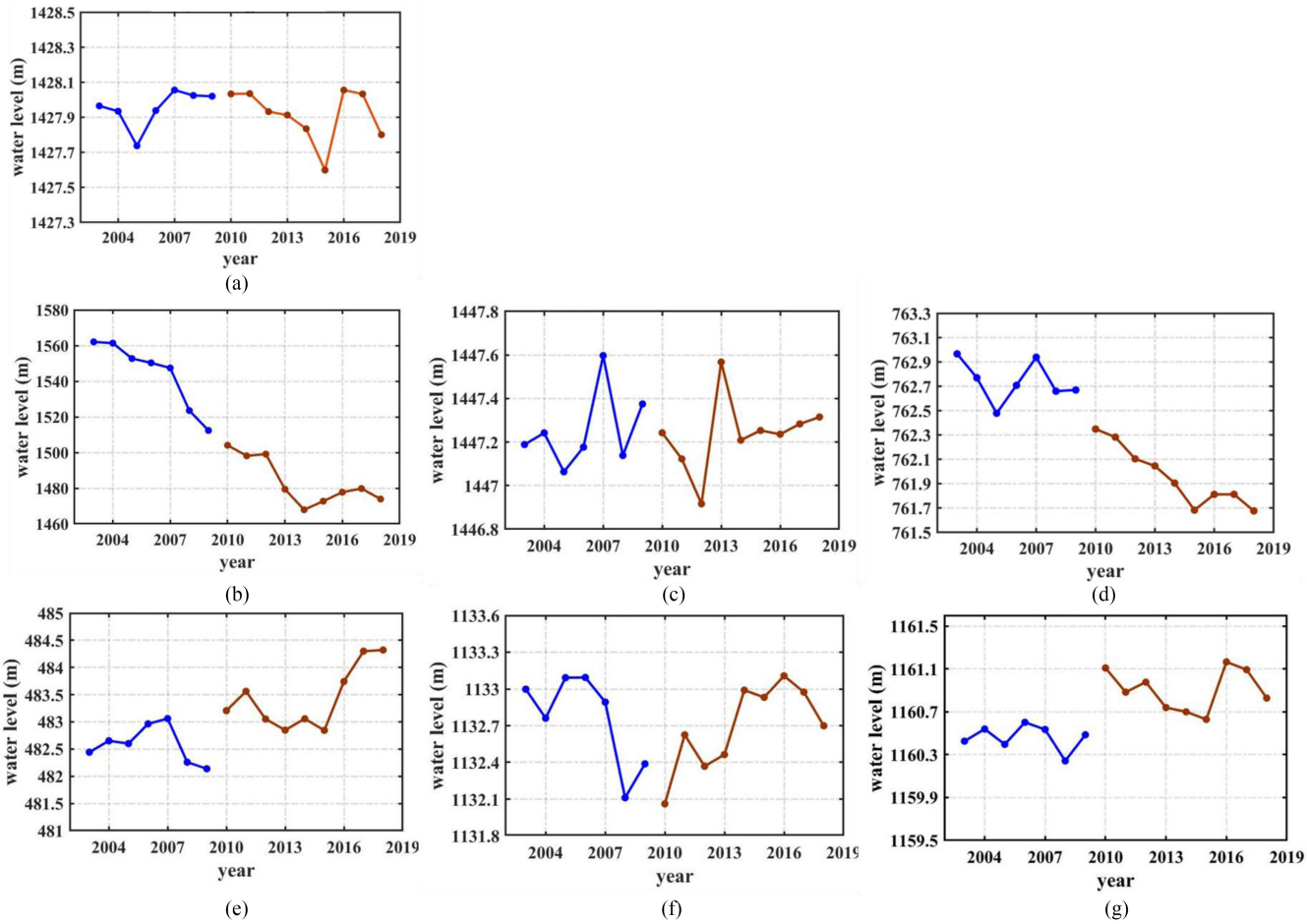

Fig. 8. Water level of seven typical lakes. The blue line represents the water level from ICESat (2003–2009) and the red line represents the water level from CryoSat-2 (2010–2018). (a) Ureg lake. (b) Hyargas. (c) Markakol lake. (d) Uvs lake. (e) Ulungu lake. (f) Hara Nurr. (g) Hara Usa.

TABLE I
WATER STORAGE CHANGE OF SEVEN LAKES

	Ureg Lake	Hyargas	Markakol	Uvs Lake	Ulungu	Hara Nurr	Hara Usa	All lake
Water storage change (2003-2009) (km^3)	0.01	-3.36	0.08	-1.06	-0.26	-0.34	0.06	-4.86
Water storage change (2010-2018) (km^3)	-0.06	-2.26	0.03	-2.41	0.96	0.36	-0.27	-3.65
Lake type	alpine closed lake	alpine closed lake	exorheic lake	alpine closed lake	plain terminal lake	exorheic lake	exorheic lake	***

occurred in Hyargas and Shaazgai Nurr with the correlation coefficient of −0.65 and −0.64, respectively. It revealed that increasing evapotranspiration is the main reason for these lakes' reduction in the east of the study region (Fig. 12).

The summer temperature change rate from 2001 to 2018 displayed an increasing trend from east to west (see Fig. 10) . The rise of temperature on lake changes not only affected the evapotranspiration but also would cause an increase of glacier melting supply. As the temperature rise, the increased glacier melting water would counteract the negative impact of the high evapotranspiration amount and cause some lakes' expansion. For example, the expanded reservoirs (ID: 37 and ID: 43) showed a significant positive correlation with the summer temperature (see Table II).

Besides, several alpine closed lakes and reservoirs showed no significant correlation with the climate factors. These lakes' variation may be caused by human activities. For example, some lakes in the east of the study region suffered reduction (such as the Tolbo lake), which may be related to the huge water demand for graziers [50]. In the Altai region, the water from the Irtysh river was diverted into some reservoirs by humans to make some contribution to some reservoirs' expansion [36].

B. *Effect of Glacial Meltwater on Lake Change*

Most of the glaciers in Altai have suffered serious shrinkage as the temperature has risen over the past few decades [51]–[53]. These glaciers are a vital freshwater source for the

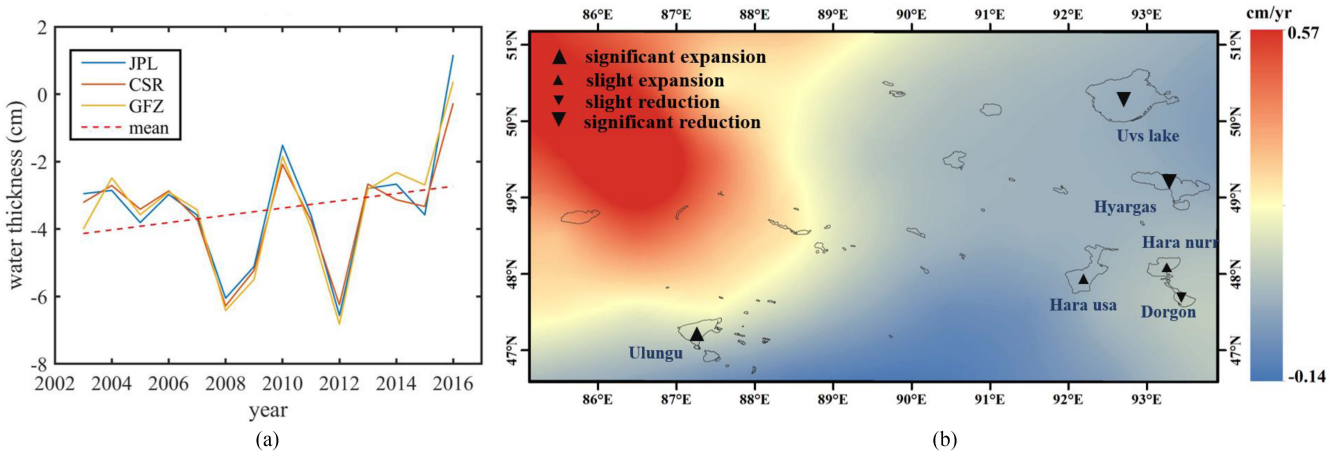

Fig. 9. (a) Annual mean TWS anomaly from three GRACE products. (b) Spatial distribution of mean annual TWS change rate with the changes in the lake area. The blue bar is the decreasing tendency, and the red bar shows the increasing tendency.

TABLE II
CORRELATION BETWEEN LAKE AREA WITH SEVERAL CLIMATE FACTORS

ID/Lake name	Lake type	Lake area change rate	ET_P	Precipitation	Temperature
Hyargas	alpine closed lake	-6.85	-0.65*	0.28	0.23
Uvs Lake	alpine closed lake	-0.48	-0.52*	0.10	0.25
Chura Usu	alpine closed lake	-0.26	-0.32	0.12	0.13
Shazzgai	alpine closed lake	-0.16	-0.64*	0.13	0.05
Tobol	alpine closed lake	-0.24	-0.34	0.07	0.18
Hara Kol	alpine closed lake	-0.01	-0.01	-0.20	0.57*
Hulagash Nurr	alpine closed lake	-0.02	0.06	0.51*	0.24
Akekul	exorheic lake	-0.02	-0.10	0.26	0.44
Dayan lake	exorheic lake	0.03	0.01	0.14	0.40
34	plain terminal lake	0.08	-0.47*	0.12	0.04
31	reservoir	0.15	-0.18	0.44	0.22
Haizikou	reservoir	-0.08	-0.46	0.20	-0.32
37	reservoir	0.52	0.16	0.41	0.55*
43	reservoir	0.30	0.20	0.16	0.62*

$*p<0.05$.

upper tributaries of the Irtysh and Ob rivers. The areas and numbers of glaciers around these lakes are decreasing from west to east, so do the lake areas. The most severe glacial recession occurred in the Katunsky, Chuysky, and Tavan Bogd, which increased runoff to the lakes in the west of the study region and counteracted the negative impact of the high evapotranspiration amount. Comparatively, the small-scale glaciers in Turgen made less contribution to the water supply in the east of the study region. The increasing evapotranspiration still caused the lakes' reduction in the east of the study region, such as Uvs lake and Hyargas. Zhang *et al*. [50] also showed that the lakes' shrinkage in the Mongolian plateau was related to the drier climate under the influence of atmospheric circulation and intensive human activities. From Fig. 13, the summer temperature showed an increasing trend in fluctuations over the past decades with the lowest summer temperatures in 2009. The lakes mainly rely on runoff from melt glaciers, and the dropped temperature would result in insufficient water supplies so that the total lake area (without Uvs and Hyargas lake) in this region shrank to its lowest level in 2009 (see Fig. 7). From 2015 to 2018, the temperature was at a relatively high and stable level, and the lake area also maintained a relatively stable trend during this period.

Previous papers illustrated that the lakes across the TP had experienced an expansion in recent decades [7], [8]. Although both the glaciers in this region and TP had a significant mass loss in the past decades, the lake water storage in the study region showed a decreasing trend. More factors need to be investigated about the impact of glacier melting water on the lake water storage considering the complex climate and unclosed hydrological cycle system in the study region [31].

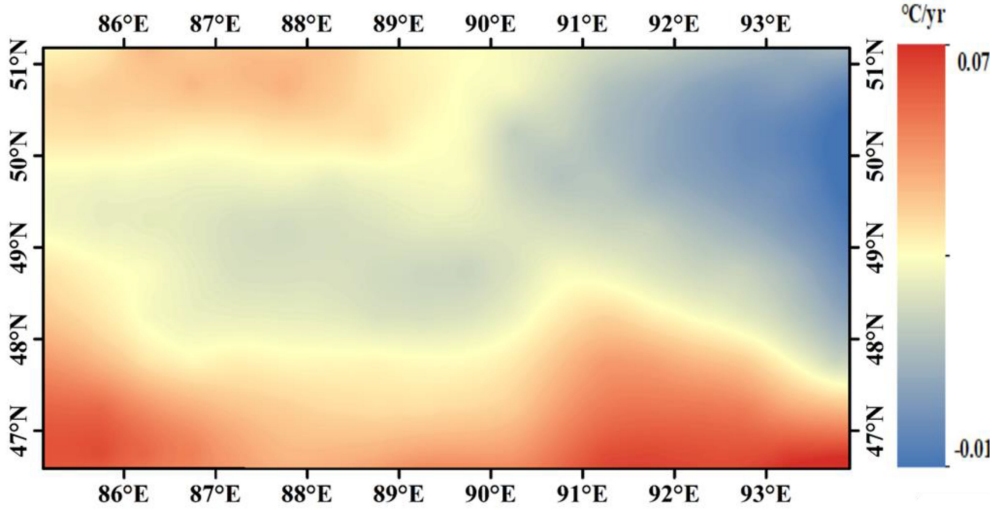

Fig. 10. Spatial trends in summer temperature across the study area.

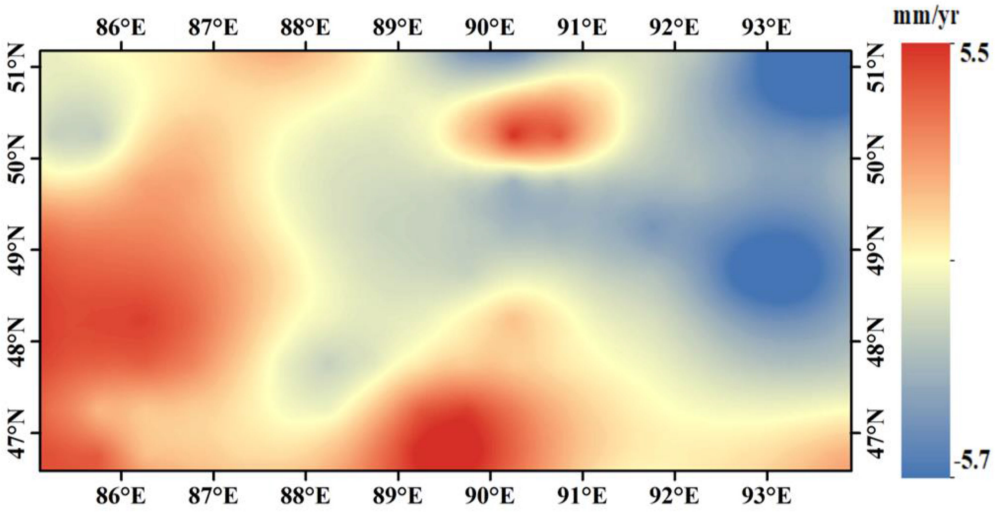

Fig. 11. Spatial trends in annual precipitation across the study area.

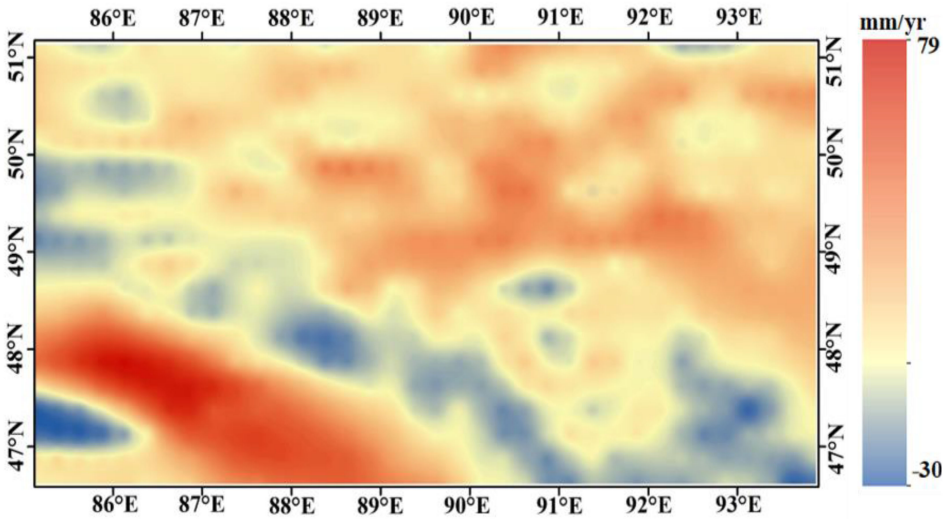

Fig. 12. Spatial trends in potential evapotranspiration across the study area.

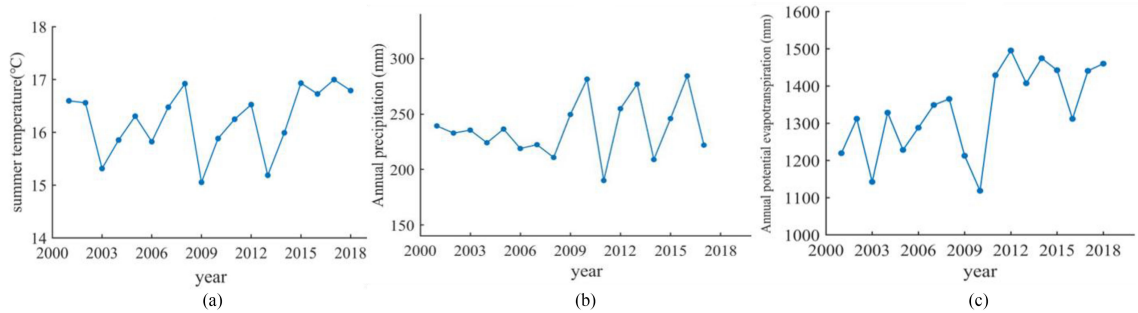

Fig. 13. (a) Annual summer temperature from 2001 to 2018. (b) Annual precipitation from 2001 to 2017. (c) Annual potential evapotranspiration from 2001 to 2018.

VI. Conclusion

In this article, the surface area of 43 lakes across the Altai mountains was investigated based on the Landsat series images. The overall lake surface area has shrunk from 9835 km^2 in 2001 to 9652 km^2 in 2009, while then rose to 9714 km^2 in 2018. By combining the lake area with the water level derived from ICESat GLAS and CryoSat-2 altimetry data, the water storage of seven lakes, accounting for 84% of the total lake area, was detected with a decrease of 4.86 ± 1.17 km^3 from 2003 to 2009 and a decrease of 3.65 ± 1.16 km^3 from 2010 to 2018, respectively. More than half of the lakes have maintained a steady water storage with insignificant upward or downward trends. The main negative balance was caused by the significant decreasing water storage of the two large lakes, i.e., Uvs and Hyargas located in the western region of the Mongolian plateau. Besides, the lake variations were analyzed in combination with climate data, including precipitation, temperature, and potential evapotranspiration.

Although most of the glaciers in this region have experienced significant mass loss in recent decades, most of the lake areas in the study region have exhibited a steady or slightly changing tendency. The reason may be that the glacial melting water in the high mountains has caused an increase in the water input and counteracted the negative impact of the high evapotranspiration amount. Despite the lakes with glacier supplies, the decreasing quantities of precipitation, high evapotranspiration, and developed animal husbandry have caused shrinkages in lakes in the western region of the Mongolian plateau, e.g., the Uvs and Hyargas lake. Further analyses in regards to the linkage between lakes and permafrost as well as the quantitative analysis about the influence of human activities would be considered as our future work.

Appendix A

TABLE III
Accuracy Level of Lake Area Extraction Compared With Google Earth Images

Lake name/id	Google Earth image data	Lake area	Landsat image data	Lake area	Kappa Coefficient	Overall accuracy	Area change ratio
Ureg Lake	2004/08/04	246.69	2004/08/28	246.67	0.96	98.6%	0.01%
Ureg Lake	2003/08/04	246.35	2003/10/05	246.78	0.96	98.4%	0.01%
Markakol Lake	2007/08/11	449.48	2007/09/11	450.34	0.99	99.5%	0.20%
Achit Lake	2013/05/13	291.70	2013/09/30	292.55	0.98	99.2%	0.29%
Achit Lake	2009/09/29	292.25	2009/08/26	292.98	0.98	99.2%	0.25%
28	2018/08/16	44.34	2018/10/12	43.74	0.97	98.9%	1.40%
Tolbo Lake	2013/12/21	79.96	2013/09/30	78.09	0.97	98.7%	2.40%
Uvs Lake	2007/08/08	3592.54	2007/06/04	3601.86	0.99	99.4%	0.30%
Khar Nurr	2006/09/07	13.67	2006/09/10	13.36	0.95	97.6%	2.30%
Shaazgai	2013/12/21	11.84	2013/09/30	12.13	0.97	99.3%	2.50%
Jili Lake	2010/07/24	168.37	2010/08/04	168.70	0.99	99.4%	0.20%
Jili Lake	2012/05/07	168.47	2012/09/02	169.45	0.97	98.6%	0.60%
Dorgan Lake	2013/06/01	554.48	2013/10/18	559.02	0.97	98.7%	0.80%
39	2009/10/14	11.34	2009/08/17	11.20	0.97	98.7%	1.20%
Tangba	2010/05/24	14.90	2010/08/04	14.60	0.95	97.7%	2.00%
Haizikou	2010/08/20	20.88	2010/09/06	20.36	0.95	97.5%	2.50%
Khar Kol	2013/10/06	7.36	2010/08/04	7.36	0.99	99.8%	0.00%
Tal Lake	2011/10/30	30.10	2011/09/16	30.39	0.99	99.7%	0.90%
Tal Lake	2016/08/13	30.29	2016/09/06	30.32	0.99	99.6%	0.07%
Tangba	2018/08/30	15.79	2016/05/24	15.74	0.98	99.6%	0.30%
Khar Nurr	2007/10/11	13.49	2007/09/29	13.35	0.98	98.9%	1.00%
Jili Lake	2006/09/30	167.60	2006/08/04	167.34	0.97	98.2%	0.20%
40	2013/04/07	8.24	2013/09/21	8.19	0.98	99.2%	0.60%
28	2013/08/02	44.49	2013/10/14	43.48	0.98	99.4%	2.10%

APPENDIX B
TABLE IV
BASIC INFORMATION ABOUT LAKES IN THE STUDY AREA

ID	Name	Latitude(°)	Longitude(°)	Lake type	Lake size
1	Hyargas	49.13	93.37	alpine closed lake	large
2	Hara Usa	48.08	92.30	exorheic lake	medium
3	Hara Nurr	48.07	93.19	exorheic lake	medium
4	Dorgon Lake	47.67	93.43	exorheic lake	medium
5	Pa-ka Hu	47.75	93.70	alpine closed lake	small
6	Uvs Lake	50.43	92.74	alpine closed lake	large
7	Chura Usu	49.11	91.89	alpine closed lake	small
8	Shaazgai Nurr	49.23	91.26	alpine closed lake	small
9	Bayan Nurr	48.83	90.92	alpine closed lake	small
10	Ureg Lake	50.11	90.99	alpine closed lake	medium
11	Achit Lake	49.46	90.55	alpine closed lake	medium
12	Achit Nor	49.35	90.62	alpine closed lake	small
13	Tolbo Lake	48.55	90.06	alpine closed lake	small
14	Dore-nor	48.23	90.66	alpine closed lake	small
15	Tal-nur	48.04	90.17	apline closed lake	small
16	Haizikou	47.17	89.74	reservoir	small
17	Dzhulu Lake	50.50	89.68	alpine closed lake	small
18	Kendikty Kul	50.34	89.82	alpine closed lake	small
19	Dund Nurr	49.48	89.79	alpine closed lake	small
20	Akekule	49.04	87.56	exorheic lake	small
21	Hara Kol	48.85	88.54	alpine closed lake	small
22	Khoton Lake	48.62	88.34	exorheic lake	small
23	Khurgan Lake	48.53	88.57	exorheic lake	small
24	Khar Nurr	48.62	88.94	alpine closed lake	small
25	Dayan Nurr	48.35	88.83	exorheic lake	small
26	Khar Nor	48.28	88.80	exorheic lake	small
27	Markakol	48.77	85.74	exorheic lake	medium
28	**	48.80	87.03	exorheic lake	small
29	Hulagash Nurr	48.32	89.15	alpine closed lake	small
30	**	47.69	87.58	reservoir	small
31	**	47.65	88.04	reservoir	small
32	**	47.64	88.21	reservoir	small
33	**	47.65	88.03	plain terminal lake	small
34	**	47.50	87.89	plain terminal lake	small
35	Ulungu	47.19	87.21	plain terminal lake	medium
36	**	47.21	87.78	plain terminal lake	small
37	**	46.64	87.73	reservoir	small
38	Jili Lake	46.91	87.40	plain terminal lake	medium
39	**	46.88	87.53	plain terminal lake	small
40	**	46.68	87.82	plain terminal lake	small
41	**	46.62	87.73	reservoir	small
42	**	46.65	87.79	reservoir	small
43	**	46.62	87.75	reservoir	small

TABLE V
LAKE AREA CHANGE AND SIGNIFICANT LEVEL IN THE STUDY AREA

ID	Name	Average lake area (2001-2008) (km^2)	Lake area change rate (2001-2008) (km^2/yr)	Lake area (2001) (km^2)	Lake area (2018) (km^2)	*p* value
1	Hyargas	1516.79	-6.85	1569.51	1473.90	<0.01***
2	Hara Usa	952.87	0.19	960.55	952.28	>0.1
3	Hara Nurr	561.54	0.09	560.88	563.02	>0.1
4	Dorgon Lake	352.34	-0.29	357.36	362.27	>0.1
5	Pa-ka Hu	6.40	-0.02	5.98	5.97	0.05-0.1*
6	Uvs Lake	3583.31	-0.48	3606.22	3572.17	<0.01***
7	Chura Usu	76.42	-0.26	78.47	73.34	<0.01***
8	Shaazgai Nurr	12.53	-0.16	13.67	11.01	<0.01***
9	Bayan Nurr	7.26	0.04	7.70	7.46	>0.1
10	Ureg Lake	246.72	0.02	246.32	246.9	>0.1
11	Achit Lake	291.54	-0.01	292.48	292.22	>0.1
12	Achit Nor	4.99	0.07	5.36	5.74	>0.1
13	Tolbo Lake	79.15	-0.24	81.61	78.28	<0.01***
14	Dore-nor	13.56	0	14.18	13.90	>0.1
15	Tal-nur	30.38	-0.03	30.73	30.29	0.01-0.05**
16	Haizikou	20.25	-0.08	21.81	19.12	0.01-0.05**
17	Dzhulu Lake	29.20	-0.01	29.41	29.19	>0.1
18	Kendikty Kul	66.03	0.03	66.54	67.35	>0.1
19	Dund Nurr	5.71	0	5.88	5.73	>0.1
20	Akekule	9.21	-0.02	9.28	8.65	0.01-0.05**
21	Hara Kol	6.17	-0.01	6.13	6.08	0.01-0.05**
22	Khoton Lake	52.86	-0.01	52.71	52.57	>0.1
23	Khurgan Lake	67.55	0.04	66.71	67.38	>0.1
24	Khar Nurr	13.38	-0.01	13.22	12.85	0.05-0.1*
25	Dayan Nurr	67.45	0.03	67.60	67.82	0.01-0.05**
26	Khar Nor	7.38	0	7.39	7.39	>0.1
27	Markakol	452.07	-0.07	452.99	450.64	>0.1
28	**	44.45	0	43.71	43.72	>0.1
29	Hulagash Nurr	5.77	-0.02	5.87	5.70	<0.01***
30	**	12.81	0.01	15.12	11.67	>0.1
31	**	4.57	0.15	4.36	6.01	<0.01***
32	**	13.91	-0.04	15.17	11.47	>0.1
33	**	5.36	-0.01	5.95	5.15	>0.1
34	**	9.47	0.08	8.73	10.28	<0.01***
35	Ulungu	849.30	0.85	848.50	862.68	0.05-0.1*
36	**	15.95	-0.21	18.52	15.88	<0.01***
37	**	19.60	0.52	13.27	22.99	<0.01***
38	Jili Lake	168.42	0.19	167.98	171.13	0.05-0.1*
39	**	14.10	0.07	14.13	15.72	>0.1
40	**	7.25	0.05	7.99	7.85	>0.1
41	**	9.15	0.21	10.63	11.19	0.01-0.05**
42	**	22.01	-0.04	24.60	20.18	>0.1
43	**	7.55	0.30	4.10	9.41	<0.01***

Lake area change rate showed the regression coefficient between the year from 2001 to 2018 and the corresponding lake area. *p*-value was associated with the significant level through M–K test. $^{*}\ p < 0.1$; $^{**}\ p < 0.05$; $^{***}\ p < 0.01$.

REFERENCES

[1] J. Z. Bai, Z. Q. Li, M. J. Zhang, W. Y. Gao, and K. M. Li, "Glacier changes in Youyi area in the Altay mountains of Xinjiang during 1959–2008," *Arid Land Geogr.*, vol. 35, pp. 116–124, 2012.

[2] A. Arendt, A. Bliss, T. Bolch, and J. G. Cogley, "Randolph glacier inventory [v4.0]: A dataset of global glacier outlines," in *Global Land Ice Measurements From Space*. Boulder, CO, USA: Springer, 2014.

[3] T. Nuimura *et al.*, "The GAMDAM glacier inventory: A quality-controlled inventory of Asian glaciers," *Cryosphere*, vol. 9, pp. 849–864, 2015.

[4] Y. Zhang, H. Enomoto, T. Ohata, H. Kitabata, T. Kadota, and Y. Hirabayashi, "Glacier mass balance and its potential impacts in the Altai mountains over the period 1990–2011," *J. Hydrol.*, vol. 553, pp. 662–677, 2017.

[5] J. W. Chipman, "A multisensor approach to satellite monitoring of trends in lake area, water level, and volume," *Remote Sens.*, vol. 11, 2019, Art. no. 158.

[6] T. Yao, Y. Wang, S. Liu, J. Pu, Y. Shen, and A. Lu, "Recent glacial retreat in high Asia in China and its impact on water resource in northwest China," *Sci. China D, Earth Sci.*, vol. 47, pp. 1065–1075, 2004.

[7] M. Walther *et al.*, "Glaciers, permafrost and lake levels at the Tsengel Khairkhan Massif, Mongolian Altai, during the late Pleistocene and Holocene," *Geosciences*, vol. 7, 2017, Art. no. 73.

[8] I. Nitze *et al.*, "Landsat-based trend analysis of lake dynamics across northern permafrost regions," *Remote Sens.*, vol. 9, 2017, Art. no. 640.

[9] X. Wang, F. Siegert, A.-G. Zhou, and J. Franke, "Glacier and glacial lake changes and their relationship in the context of climate change, central Tibetan plateau 1972–2010," *Global Planet. Change*, vol. 111, pp. 246–257, 2013.

[10] G. Veh, O. Korup, S. Roessner, and A. Walz, "Detecting Himalayan glacial lake outburst floods from landsat time series," *Remote Sens. Environ.*, vol. 207, pp. 84–97, 2018.

[11] Y. Ma, N. Xu, J. Sun, X. H. Wang, F. Yang, and S. Li, "Estimating water levels and volumes of lakes dated back to the 1980s using landsat imagery and photon-counting lidar datasets," *Remote Sens. Environ.*, vol. 232, 2019, Art. no. 111287.

[12] S. Lu, B. Wu, N. Yan, and H. Wang, "Water body mapping method with HJ-1A/B satellite imagery," *Int. J. Appl. Earth Observ. Geoinf.*, vol. 13, pp. 428–434, 2011.

[13] W. Shanrong, "Study on tends of lakes variation in Qaidam basin," M.S. thesis, China Univ. Geosci., Wuhan, China, 2016.

[14] Y. Zhou, L. Zhang, and Y. Wang, "Monitoring of water extent and variation of the Poyang lake using GF-1 remote sensing data," in *Proc. 7th Int. Conf. Manuf. Sci. Eng.*, Apr. 2017, pp. 384–387.

[15] L. Jiang, K. Nielsen, O. B. Andersen, and P. Bauer-Gottwein, "CryoSat-2 radar altimetry for monitoring freshwater resources of China," *Remote Sens. Environ.*, vol. 200, pp. 125–139, 2017.

[16] C. Yuan, P. Gong, H. Zhang, H. Guo, and B. Pan, "Monitoring water level changes from retracked Jason-2 altimetry data: A case study in the Yangtze river, China," *Remote Sens. Lett.*, vol. 8, pp. 399–408, 2017.

[17] L. Jiang, K. Nielsen, O. B. Andersen, and P. Bauer-Gottwein, "Monitoring recent lake level variations on the Tibetan plateau using cryoSat-2 SARIn mode data," *J. Hydrol.*, vol. 544, pp. 109–124, 2017.

[18] J. Li, X. Chen, and A. Bao, "Spatial-temporal characteristics of lake level changes in central Asia during 2003–2009," *Acta Geographica Sinica*, vol. 66, pp. 1219–1229, 2011.

[19] G. Zhang, H. Xie, S. Kang, D. Yi, and S. F. Ackley, "Monitoring lake level changes on the Tibetan plateau using ICESat altimetry data (2003–2009)," *Remote Sens. Environ.*, vol. 115, pp. 1733–1742, 2011.

[20] C. Song, Q. Ye, and X. Cheng, "Shifts in water-level variation of Namco in the central Tibetan plateau from ICESat and CryoSat-2 altimetry and station observations," *Sci. Bull.*, vol. 60, pp. 1287–1297, 2015.

[21] D. Long *et al.*, "Deriving scaling factors using a global hydrological model to restore GRACE total water storage changes for China's Yangtze river basin," *Remote Sens. Environ.*, vol. 168, pp. 177–193, 2015.

[22] Z. Zhang, B. F. Chao, J. Chen, and C. R. Wilson, "Terrestrial water storage anomalies of Yangtze river basin droughts observed by GRACE and connections with ENSO," *Global Planet. Change*, vol. 126, pp. 35–45, 2015.

[23] D. Long *et al.*, "Drought and flood monitoring for a large karst plateau in southwest China using extended GRACE data," *Remote Sens. Environ.*, vol. 155, pp. 145–160, 2014.

[24] H. Chen, W. Zhang, N. Nie, and Y. Guo, "Long-term groundwater storage variations estimated in the Songhua river basin by using GRACE products, land surface models, and in-situ observations," *Sci. Total Environ.*, vol. 649, pp. 372–387, 2019.

[25] M. Khaki and J. Awange, "The application of multi-mission satellite data assimilation for studying water storage changes over South America," *Sci. Total Environ.*, vol. 647, pp. 1557–1572, 2019.

[26] K. Yang *et al.*, "Recent dynamics of Alpine lakes on the endorheic Changtang plateau from multi-mission satellite data," *J. Hydrol.*, vol. 552, pp. 633–645, 2017.

[27] S. Yi, Q. Wang, L. Chang, and W. Sun, "Changes in mountain glaciers, lake levels, and snow coverage in the Tianshan monitored by GRACE, ICESat, altimetry, and MODIS," *Remote Sens.*, vol. 8, 2016, Art. no. 798.

[28] G. Zhang *et al.*, "Response of Tibetan plateau lakes to climate changes: Trend, patterns, and mechanism," *Earth-Sci. Rev.*, vol. 208, 2020, Art. no. 103269.

[29] C. Song, B. Huang, and L. Ke, "Modeling and analysis of lake water storage changes on the Tibetan plateau using multi-mission satellite data," *Remote Sens. Environ.*, vol. 135, pp. 25–35, 2013.

[30] P. Moore and S. D. P. Williams, "Integration of altimetric lake levels and GRACE gravimetry over Africa: Inferences for terrestrial water storage change 2003–2011," *Water Resour. Res.*, vol. 50, pp. 9696–9720, 2014.

[31] A. Frampton, S. Painter, S. W. Lyon, and G. Destouni, "Non-isothermal, three-phase simulations of near-surface flows in a model permafrost system under seasonal variability and climate change," *J. Hydrol.*, vol. 403, pp. 352–359, 2011.

[32] N. Malygina, A. N. Eirich, T. V. Barlyeva, and T. Papina, "Isotope composition of macrocirculation processes responsible for precipitation in the Altai mountains," *IOP Conf., Earth Environ. Sci.*, vol. 211, 2018, Art. no. 012008.

[33] V. B. Aizen, E. M. Aizen, D. R. Joswiak, K. Fujita, N. Takeuchi, and S. A. Nikitin, "Climatic and atmospheric circulation pattern variability from ice-core isotope/geochemistry records (Altai, Tien Shan and Tibet)," *Ann. Glaciol.*, vol. 43, pp. 49–60, 2006.

[34] M. Klinge, J. Böhner, and F. Lehmkuhl, "Climate pattern, snow and timberlines in the Altai mountains, Central Asia," *Erdkunde*, vol. 57, pp. 296–308, 2003.

[35] N. Malygina, T. Papina, N. Kononova, and T. Barlyaeva, "Influence of atmospheric circulation on precipitation in Altai mountains," *J. Mountain Sci.*, vol. 14, pp. 46–59, 2017.

[36] I. Bayer, "Analysis on recent changes of surface water resources of the Ulungur lake based on RS technology," Xinjiang Normal Univ., Ürümqi, China, 2013.

[37] S. Swenson and J. Wahr, "Post-processing removal of correlated errors in GRACE data," *Geophys. Res. Lett.*, vol. 33, 2006, Art. no. L08402.

[38] M. Cheng and B. D. Tapley, "Variations in the earth's oblateness during the past 28 years," *J. Geophys. Res., Solid Earth*, vol. 109, 2004, Art. no. B09402.

[39] A. Geruo, J. Wahr, and S. Zhong, "Computations of the viscoelastic response of a 3-D compressible earth to surface loading: An application to glacial isostatic adjustment in Antarctica and Canada," *Geophys. J. Int.*, vol. 192, pp. 557–572, 2013.

[40] M. Rodell *et al.*, "The global land data assimilation system," *Bull. Amer. Meteorol. Soc.*, vol. 85, pp. 381–394, 2004.

[41] W. Feng, M. Zhong, J.-M. Lemoine, R. Biancale, H.-T. Hsu, and J. Xia, "Evaluation of groundwater depletion in north China using the gravity recovery and climate experiment (GRACE) data and ground-based measurements," *Water Resour. Res.*, vol. 49, pp. 2110–2118, 2013.

[42] B. R. Scanlon *et al.*, "Groundwater depletion and sustainability of irrigation in the US high plains and central valley," *Proc. Nat. Acad. Sci.*, vol. 109, pp. 9320–9325, 2012.

[43] S. K. McFeeters, "The use of the normalized difference water index (NDWI) in the delineation of open water features," *Int. J. Remote Sens.*, vol. 17, pp. 1425–1432, 1996.

[44] A. Frankl, A. Zwertvaegher, J. Poesen, and J. Nyssen, "Transferring google earth observations to GIS-software: Example from gully erosion study," *Int. J. Digit. Earth*, vol. 6, pp. 196–201, 2013.

[45] F. E. O'Loughlin, J. Neal, D. Yamazaki, and P. D. Bates, "ICESat-derived inland water surface spot heights," *Water Resour. Res.*, vol. 52, pp. 3276–3284, 2016.

[46] J. Benveniste, V. Rosmorduc, S. Niemeijer, and N. Picot, "Basic radar altimetry toolbox," in *Proc. IEEE Int. Geosci. Remote Sens. Symp.*, 2008, pp. 895–898.

[47] B. Zhang, Y. Wu, L. Zhu, J. Wang, J. Li, and D. Chen, "Estimation and trend detection of water storage at Nam Co lake, central Tibetan plateau," *J. Hydrol.*, vol. 405, pp. 161–170, 2011.

[48] J. C. Schneider, *Manual of Fisheries Survey Methods II: With Periodic Updates*. Lansing, MI, USA: Michigan Dept. Natural Resour., Fisheries Division, 2000.

[49] S. Yue, P. Pilon, and G. Cavadias, "Power of the Mann–Kendall and Spearman's rho tests for detecting monotonic trends in hydrological series," *J. Hydrol.*, vol. 259, pp. 254–271, 2002.

[50] G. Zhang *et al.*, "Extensive and drastically different Alpine lake changes on Asia's high plateaus during the past four decades," *Geophys. Res. Lett.*, vol. 44, pp. 252–260, 2016.

[51] Y. Narozhniy and V. Zemtsov, "Current state of the Altai glaciers (Russia) and trends over the period of instrumental observations 1952–2008," *Ambio*, vol. 40, pp. 575–588, 2011.

[52] U. Kamp and C. G. Pan, "Inventory of glaciers in Mongolia, derived from landsat imagery from 1989 to 2011," *Geografiska Annaler A, Phys. Geogr.*, vol. 97, pp. 653–669, 2015.

[53] B. S. Krumwiede, U. Kamp, G. J. Leonard, J. S. Kargel, A. Dashtseren, and M. Walther, "Recent glacier changes in the Mongolian Altai mountains: Case studies from Munkh Khairkhan and Tavan Bogd," in *Global Land Ice Measurements From Space*. Berlin, Germany: Springer, 2014, pp. 481–508.

[54] M. A. Faiz *et al.*, "How accurate are the performances of gridded precipitation data products over northeast China?," *Atmos. Res.*, vol. 211, pp. 12–20, 2018.

[55] X. Zhu *et al.*, "Comparison of monthly precipitation derived from high-resolution gridded datasets in arid Xinjiang, Central Asia," *Quaternary Int.*, vol. 358, pp. 160–170, 2015.

[56] Y. Zhang, B. He, L. Guo, J. Liu, and X. Xie, "The relative contributions of precipitation, evapotranspiration, and runoff to terrestrial water storage changes across 168 river basins," *J. Hydrol.*, vol. 579, 2019, Art. no. 124194.

[57] L. Mokgedi, J. Nobert, and S. Munishi, "Assessment of lake surface dynamics using satellite imagery and in-situ data; case of lake Ngami in north-west Botswana," *Phys. Chem. Earth, A/B/C*, vol. 112, pp. 175–186, 2019.
[58] S. Berezovskaya, D. Yang, and D. L. Kane, "Compatibility analysis of precipitation and runoff trends over the large Siberian watersheds," *Geophys. Res. Lett.*, vol. 31, 2004, Art. no. L21502.
[59] C. Vera, G. Silvestri, B. Liebmann, and P. González, "Climate change scenarios for seasonal precipitation in South America from IPCC-AR4 models," *Geophys. Res. Lett.*, vol. 33, 2006, Art. no. L13707.
[60] E. D. Coffel *et al.*, "Future hot and dry years worsen Nile basin water scarcity despite projected precipitation increases," *Earth's Future*, vol. 7, pp. 967–977, 2019.
[61] C. J. Willmott and K. Matsuura, "Terrestrial air temperature and precipitation: Monthly and annual time series (1950–1999)," Center Climatic Res., Dept. Geogr., Univ. Delaware, Newark, DE, USA, 2001.

Rong Luo received the B.S. degree in geodesy and geomatics engineering, in 2018 from Wuhan University, Wuhan, China, where she is currently working toward the M.S. degree in photogrammetry and remote sensing with the School of Geodesy and Geomatics.

Her research interests include remote sensing image processing and application, and data fusion.

Qiangqiang Yuan (Member, IEEE) received the B.S. degree in surveying and mapping engineering and the Ph.D. degree in photogrammetry and remote sensing from Wuhan University, Wuhan, China, in 2006 and 2012, respectively.

In 2012, he joined the School of Geodesy and Geomatics, Wuhan University, Wuhan, China, where he is currently an Associate Professor. He has authored or coauthored more than 70 research papers, including more than 50 peer-reviewed articles in international journals, such as the IEEE TRANSACTIONS ON IMAGE PROCESSING and IEEE TRANSACTIONS ON GEOSCIENCE AND REMOTE SENSING. His current research interests include image reconstruction, remote sensing image processing and application, and data fusion.

Dr. Yuan was a recipient of the Youth Talent Support Program of China, in 2019, the Top-Ten Academic Star of Wuhan University, in 2011, and the Hong Kong Scholar Award from the Society of Hong Kong Scholars and the China National Postdoctoral Council, in 2014. He is an Associate Editor for the IEEE *Access* journal and has frequently served as a referee for more than 40 international journals for remote sensing and image processing.

Linwei Yue received the B.S. degree in geographic information system and the Ph.D. degree in photogrammetry and remote sensing from Wuhan University, Wuhan, China, in 2012 and 2017, respectively.

She was an Associate Professor with the School of Geography and Information Engineering, China University of Geosciences, from 2017. Her research interests include multisource remote sensing data fusion and hydrological applications.

Xiaogang Shi (Member, IEEE) received the M.Sc. degree in water resources engineering from McMaster University, Hamilton, ON, Canada, in 2005, and the Ph.D. degree in hydrology and water resources from the University of Washington, Seattle, WA, USA, in 2013.

He is currently a Senior Lecturer in hydrology with the University of Glasgow, Glasgow, Scotland. Since 2020, he has been with the interdisciplinary research theme leadership team of sustainability with the College of Social Sciences. Prior to joining the University of Glasgow, in 2018, he was a Lecturer with Lancaster University and Xi'an Jiaotong-Liverpool University, and a Research Scientist with the Commonwealth Scientific and Industrial Research Organisation, Canberra, ACT, Australia.

Dr. Shi was a recipient of the postdoctoral fellowship Natural Sciences and Engineering Research Council of Canada and the Research Innovation Award of Australian Water Association, in 2015.